NASA TECHNICAL MEMORANDUM

NASA TM-78845

NASA TM-78845

IMPACT BEHAVIOR OF FILAMENT WOUND GRAPHITE/EPOXY FAN BLADES

by Kenneth J. Bowles
Lewis Research Center
Cleveland, Ohio 44135

TECHNICAL PAPER to be presented at the
Twenty-third National SAMPE Symposium and Exhibition
Anaheim, California, May 2-4, 1978

IMPACT BEHAVIOR OF FILAMENT-WOUND GRAPHITE/EPOXY FAN BLADES

Kenneth J. Bowles
National Aeronautics and Space Administration
Lewis Research Center
Cleveland, Ohio

Abstract

The fabrication and impact tests of graphite/epoxy filament wound fan blades are discussed. Blades which were spin tested at tip speeds up to 305 meters per second retained their structural integrity. Two blades were each impacted with a 454 gram slice of a 908 gram simulated bird at a tip speed of 263 meters per second and impact angles of 22° and 32°. The impact tests were recorded with high-speed movie film. The blade which was impacted at 22° sustained some root delamination but remained intact. The 32° impact separated the blade from the root. No local damage other than leading-edge debonding was observed for either blade. The results of a failure mode analysis are also discussed.

E-9562

1.0 INTRODUCTION

A significant amount of work has been directed toward the evaluation of resin matrix/fiber reinforced composites for the low temperature components of turbofan aircraft engines. It has been shown[1] that improvements in the overall engine performance can be realized by the use of these materials. The substitution of resin matrix/fiber reinforced composites for metal fan blades, metal fan frames, metal nacelles and early stage metal compressor blades can result in a decrease in the engine weight and specific fuel consumption. Of the low temperature engine components, the fan blade has been the component undergoing the major amount of study and testing because of the foreign object damage (FOD) ingestion re-

quirements that it must meet.

The conventional method used to fabricate composite engine fan blades is to build them up from individual unidirectional plies of prepreg material. The individual plies are oriented at various angles to produce "tailor-made" directional mechanical strength properties as required by the specific blade design. For this type of fabrication, prepreg tape or broadgoods must be used. The individual plies with the proper fiber orientation are cut from the prepreg material and then precisely stacked to produce the required blade form for molding and curing. A filament winding method of fabricating spar shell blades has been developed.[2] It has the potential of reducing the costs of fabricating resin matrix composite fan blades.

The purpose of this report is to describe the results of spin and foreign object impact tests that were conducted on filament wound blades. Two blades were spin tested to proof test the pinned root design of the blade and two blades were impacted with simulated birds to determine the effect of the filament wound construction on the blade FOD resistance.

2.0 BLADE DESIGN

An illustration of the blade construction is shown schematically in Figure 1. The blade was fabricated in a spar shell configuration from Thornel 300 graphite fiber impregnated with APCO 2434/2437 epoxy resin.

The unidirectional 0^{o} spar filaments were continuous and extended from the tip of the blade down the length of the blade around the metal root bushing and up the other side of the blade to the tip of the blade. The root of the blade was of a pin root design. The continuous longitudinal fibers had to withstand the tensile forces resulting from the spinning of the blade. They also had to withstand the shear forces of the metal bushing which pressed against the sides of the fibers where they were wrapped around the bottom of the bushing.

Alternating layers of fiberglass cloth laminae were laid between the longitudinal graphite fibers in the root area to increase the shear resistance in the root. This produced a lower root composed of graphite fibers and fiberglass laminae. The outermost layer was fiberglass.

The blade airfoil was encased in a 0.086 cm thick graphite/epoxy filament wound shell with a $\pm 45^{o}$ fiber orientation.

The shell fibers were continuous except at the blade tip and the root termination point. Two blades were fabricated with a Type 301 stainless steel leading edge protection shield.

The blades had a span of 57.15 cm measured from the root pin axis to the blade tip. The chord was 15.25 cm at the tip. There was no axial taper to the blade and the twist was 45^{o} from the pin to the tip.

3.0 FABRICATION PROCEDURE

The fabrication steps used in fabricating the blades were as follows:

(1) Spar winding
(2) $\pm 45^{o}$ Shell winding
(3) Positioning in the mold
(4) Curing
(5) Trimming
(6) Finishing

Spar winding consisted simply of winding the graphite fibers over two metal spool pieces which were separated by a distance equal to the sum of two blade lengths plus 10.2 cm. The fiber bundles were spread at the midpoint of the two spool pieces to obtain the required chordwise contour of the blades.

After the spar winding had been completed, the spar-spool assembly was sealed inside of an adhesive film bag. The bag was pressurized with air, transferred to a winding machine and overwrapped with the $\pm 45^{o}$ shell. (See Fig. 2.)

After the completion of the shell winding step, the two-blade assembly was positioned in the mold. The adhesive film bag was deflated and the blade cured.[2]

After the curing step, the blade pair was removed from the mold, trimmed (see Fig. 3) and then the two blades were separated and finished (Fig. 4). Four blades were fabricated designated FS-1, 2, 3, and 4. Metal protection sheaths were bonded in place on blades FS-3 and FS-4 with epoxy resin.

4.0 EXPERIMENTAL PROCEDURES

4.1 SPIN TEST

The spin tests were conducted in a rotating arm test rig at Hamilton Standard, Windsor Locks, Connecticut. Figure 5 shows the rig with a blade installed. A detailed description of the facility is given in Reference 3.

The test cell was evacuated to an air pressure of 1.04×10^{4} N/m^{2} (1.5 psia) to minimize air friction heating during the spin tests. Blade surface temperatures were monitored by Tempilar temperature sensitive paint which was applied to the

surface of the blade before each test. The cell temperature was monitored using a thermocouple. The temperature limit was set at 93.5° C (200° F) for the cell and 121° C (250° F) for the blade.

Each of the two blades was tested at five tip speeds. A speed of 304.8 m/sec (1000 ft/sec) was the maximum test speed (11 percent greater than design). The four other speeds were 50, 75, 90, and 95 percent of the maximum test speed.

The lower speed tests were conducted for 30 seconds. The spin test at maximum speed of 304.8 m/sec was run for a total time of 5 minutes. For both blades the maximum speed test time was an accumulated time of three separate runs. This was necessary because at this speed the cell temperature rose to 93.5° C (200° F) within $1\frac{1}{2}$ to 2 minutes after test start time. The seven speed cycles and the time at each speed was considered to adequately test the structural integrity of each blade.

Each blade was tap tested with a metal hammer at the conclusion of each spin test run. Blade FS-2 was sectioned and examined after the series of runs was completed.

4.2 FOD TESTS

Uninstrumented impact tests were performed on the two blades (FS-3 and FS-4) which had metal leading edge protection sheaths. The test facility was the same G-5 whirling arm test rig that was used for the spin tests. The blades were impacted by simulated birds at a point located at 0.8 of the span of the blade. Blade tip speeds were 263 meters per second.

The simulated birds weighed 908 gms and were formed from a mixture of gelatin, water, and phenolic microballons. The mixture was proportioned to produce a specific gravity of 0.69. The birds were cylindrical in shape with a length to diameter ratio of two. Figure 6 shows a dimensional sketch of the simulated bird.

The target simulated bird slice size for the two impact tests was 454 gms. The exact weight of the slice was determined by the difference in the weights of the bird before and after impact. Two impact incidence angles were chosen for the tests. One impact was made at an angle of 22° with the leading edge of the blade. This corresponds to the calculated angle of impact at cruise speeds. The second blade was impacted at an angle of 32°

which is the calculated angle of impact expected under the full power conditions experienced during takeoff.

The impact events were recorded on film by two high-speed movie cameras. One camera was focused at the tip of the blade in line with the longitudinal axis of the blade airfoil as the blade passed through the impact arc of about 25°. The second camera was focused on the pressure surface of the blade airfoil from an angle of about 30° to the airfoil surface.

During the calibration of the simulated bird injection apparatus prior to the 22° impact test, the leading edge of blade FS-3 accidentally struck the bird injection apparatus stand. Some damage was sustained by the blade. Radial cracking of the spar near the leading edge (Fig. 7), shell debonding (Fig. 7) and leading edge protection sheath debonding (Fig. 8) were evident. Visual examination of the blade and tap tests (hand tapping at several span locations with a hammer) indicated that the damage was confined to the upper 20 percent of the blade span and the test was continued.

5.0 METHODS OF ANALYSIS

5.1 ANALYSIS OF SPIN TESTED BLADES

Blades FS-1 and FS-2 were tap tested between test spins and at the conclusion of the tests. The tap testing indicated that neither blade suffered structural degradation from the forces generated by spinning. To confirm this qualitative test, blade FS-2 was sectioned and examined using a dye penetrant method.

5.2 ANALYSIS OF IMPACTED BLADE

The reaction of the blades to the impacts were measured from the filmed sequences of the impacts. Blade tip angles and blade tip deflections were measured from projections of individual frames of the impact events.

Blade FS-3 was sectioned after it was impacted and was dye penetrant checked to determine the nature and extent of damage caused by the impact.

6.0 RESULTS

6.1 BLADE FS-3 (22° IMPACT)

Blade FS-3 was impacted at an angle of 22° with the simulated bird. The slice size was 449 gms. The blade remained intact after the impact. Figures 9(a), 10(a), 11 and 12 show the blade after the impact. When these figures are compared with Figures 7 and 8

it can be seen that the leading edge protection sheath completely debonded along the suction face of the airfoil but not the pressure side. The amount of radial cracking in the spar tip did not increase significant'y. The delamination of the shell from the spar at the tip of the blade (line B-B, Fig. 12) is about 2.54 cm to the left of the dashed line (A-A) in Figure 12. This increase was about 5 percent of the airfoil pressure face surface. Visual examination of the bl ide root showed that some root damage also occurred. The fiberglass root overlay was debonded from the wedge shaped sides of the root and there were some tears in the fiberglass in the corners where the 15.2 cm airfoil chord joined the 7.6 cm wide root.

The blade was sectioned and examined with dye penetrant. The results can be seen in Figure 13. Insets A and B show the blade tip and a section through the area of impact. Some radial cracking of the spar is evident. These cracks, when compared to the cracks shown in Figure 7, appear to be caused when the blade accidentally struck the injection apparatus stand prior to testing. No significant local damage was revealed by examination of these two sections.

Inset C of Figure 13 reveals the first example of blade damage caused by the simulated bird impact. A shear type of crack can be seen near the trailing edge of the blade. Progressing down the blade (insets D, E, and F) it can be seen that the crack lengthens across the chord of the blade. Also, radial cracking of the spar is evident. Insets G, H, J, and K show that the crack extends down into the root of the blade.

A frame-by-frame analysis of the high-speed camera film provided enough information to obtain a good understanding of the reaction of the blade tip to the impact. As the leading edge of the blade passed through the simulated bird, the angle of the blade tip remained unchanged. When the leading edge of the blade started to emerge from the bird, the blade tip began twisting so as to increase the angle of incidence between the blade and the bird. This twisting continued until the trailing edge of the blade started passing through the bird. Then the twisting reversed. The films showed that blade twisting was initiated by two sharp impacts. One was against the leading

half of the blade and the other was against the trailing half of the blade. Evidence of two such heavy impacts can be seen in Figure 12. Two darkened scuff marks are visible on the surface of the blade. One is near the leading edge and the second extends along most of the trailing half of the blade. Blade tip angle measurements and times of measurement are presented in Table 1.

6.2 BLADE FS-4 (32° IMPACT)

Blade FS-4 was impacted with a 409 gm (0.916) slice of the simulated bird. As a result of the impact, the blade airfoil separated from the blade root (Figs. 9(b), 10(b), and 14) and impacted with the cell wall at a point 180° from the point of impact with the bird. Since the airfoil was pulverized by the impact with the cell wall, it was unavailable for sectioning. Figures 9(b) and 14 show the pressure face of the blade root after the impact. The fiberglass overlay was completely removed from the surface of the angled transition section. Spar fiber breakage extended to where curvature around the pin bushing begins, near the leading edge of the pressure side of the blade root. On the suction side of the blade root, all spar fibers broke where the fiberglass overlay terminated on the lower part of the airfoil.

Examination of the root transition area revealed that approximately 33 percent of the spar fibers that were wound around the bushing were ineffective. The fibers were cut during the root trimming step of blade fabrication because they had not been properly positioned. The cutting of the fibers significantly reduced the load bearing capacity of the root section.

Analysis of the motion pictures showed that blade FS-4 experienced the same chordwise twisting as blade FS-3. The data are shown in Table 2. Figure 15 shows a schematic description of the reaction of the blade tip to the impact. All views are superimposed on the same reference plane. The solid tip outline indicates the position of the blade tip as the blade was about to contact the bird. The dashed tip outline shows the position of maximum twist of the blade tip that occurred at the time the trailing edge of the blade impacted the simulated bird. The dotted tip outline indicates the position of the blade tip as it was leaving the viewing area of the camera. The first impact (leading edge) started the blade twist-

ing. The second impact stopped the twisting but did not reverse it as with blade FS-3. Instead of a reverse twist, the blade bent backwards with the leading edge fibers having been strained much more severely than the trailing edge fibers.

The only sign of local damage which could be observed from the films was a complete separation of the leading edge sheath from the airfoil as the blade impacted the bird.

7.0 DISCUSSION OF RESULTS

7.1 SPIN TESTS

The results of the spin tests show that the pin-root design, which could be adapated easily to unidirectional spar winding techniques, possessed the structural characteristics it was designed to have. Both blades were spun to tip speeds 11 percent greater than the design tip speed with no degradation of the structural integrity of either blade. The blades were both tested by tap testing at the conclusion of the spin tests and one blade was examined by sectioning. The results of these tests showed that the two blades successfully withstood the centrifugal forces of spinning.

7.2 IMPACT TESTS

Previous FOD testing of ply layup blades has shown that some local impact damage (leading edge failure) is initiated during the time interval that the blade is in contact with the simulated bird (ref. 4). Under the impact conditions chosen for these tests, neither of the two blades suffered any significant local impact damage other than debonding of the leading edge protection sheath. The pnotos of the cross sections of blade FS-3 (Fig. 13) provided additional data to support this finding. The top right hand photograph (Section B) shows a cross section of the blade airfoil at the plane of impact. Delaminations are not visible; only radial cracks can be seen. The area of shell delamination at the tip of blade FS-3 caused by the accidental impact of the blade with the bird injection stand was increased by the 22° impact. The delamination increased only about 5 percent of the airfoil surface.

The impact of blade FS-3 with the simulated bird at an angle of 22° was sufficient to initiate some damage in the root area of the blade. The damage is shown in Figure 13

(insets D, E, and F) and consists of what appears to be a shear failure at the neutral axis of the blade spar. The blade twisting alone did not cause this failure.

It was observed that when the blade FS-4 was impacted at an angle of 32° with the simulated bird, the same sequence of events occurred. The blade started twisting with the leading edge moving backward and there were indications of a second impact in the trailing half of the blade. Pronounced backward bending of the leading edge tip was also observed with the fibers in the tip of the leading edge being displaced farther than the fibers in the tip of the trailing edge.

7.3 RECOMMENDATIONS

In order to improve the structural integrity of the root, some obvious improvements can be made to this blade.

The wrap around plies of fiberglass fabric used in building up the root, while strengthening the root against tensile forces, did not increase the resistance to shear or transverse tensile loading. Fabric oriented parallel to the longitudinal spar filaments through the thickness of the root could possibly increase the shear and transverse tensile strengths in this area.

While the blade airfoil was completely encased within a $\pm 45^{\circ}$ shell of wound fibers, the root area was not. The $\pm 45^{\circ}$ fibers covered only the suction and pressure faces of the root. The wedge shaped sides were trimmed after curing and the angled fibers were cut away. Epoxy impregnated fiberglass was wrapped over the root area to provide reinforcement, but the fiberglass tore at the sharp corners in both impact tests. The glass reinforcement may have been more effective had these corners been rounded.

A more positive method of aligning the spar fibers in the root area would assure that the fabricated blade root would possess the actual strength it was designed to have. A fabrication process should be developed which does not require trimming in the root area so that both the radial strength of the spar fibers and the torsional strength of the shell fibers could be utilized in the root.

8.0 SUMMARY OF RESULTS AND CONCLUSIONS

Based on the results of this investigation, the following conclusions can be made:

1. A filament wound root can be designed to withstand the

centrifugal forces of spinning.

2. The filament wound blade investigated in this study withstood a 22° impact with a 454 gm slice of a 908 gm simulated bird. Some root damage did occur. There was no loss of blade material other than the leading edge sheath.

3. The blade root as designed for this study could not withstand a 32° impact with a 454 gm slice of a 908 gm simulated bird.

4. Failures in the root sections were initiated by shear and/or transverse tensile forces from blade bending.

9.0 REFERENCES

1. Steinhagen, C. A.; Stotler, C. L.; and Neitzel, R. E.: Study of the Costs and Benefits of Composite Materials in Advanced Turbofan Engines (R74AEG18, General Electric Company; NAS3-17775) NASA CR-134696, 1974.

2. Yao, Sam: Filament Wound Spar Shell Graphite/Epoxy Fan Blades (FSI-551-201, Fiber Science, Inc.; NAS3-17822) NASA CR-134899, 1976.

3. Graff, J.; Stoltze, L.; and Varholak, E. M.: Impact Resistance of Spar Shell Composite Fan Blades. (HSER-6241, Hamilton Standard; NAS 3-16788) NASA CR 134521, 1973.

4. Impact Resistance of Composite Fan Blades. (R74AEG320, General Electric; NAS3-16777) NASA CR 134707, December 1974.

Table 1. Blade Tip Reaction From 22° Impact

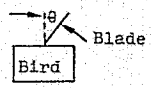

Time, sec	Tip chord angle, θ, deg	Remarks
0	17.5	Blade leading edge 2.1 cm from exiting bird
9.1×10^{-5}	20.0	Blade leading edge exiting bird
18.2×10^{-5}	20.5	
27.3×10^{-5}	22.5	
36.4×10^{-5}	25.5	
45.5×10^{-5}	25.5	Trailing edge hits bird
54.6×10^{-5}	22.5	
63.7×10^{-5}	20.0	

Table 2. Blade Tip Reaction From 32° Impact

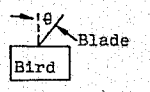

Time, sec	Tip chord angle, θ, deg	Remarks
0	27.5	Leading edge 2.1 cm from exiting bird
9.1×10^{-5}	34.0	Blade leading edge exiting bird
18.2×10^{-5}	38.5	Trailing edge hits bird
27.3×10^{-5}	45.5	
36.4×10^{-5}	45.5	
45.5×10^{-5}	46.0	
54.6×10^{-5}	48.5	
63.7×10^{-5}	50.0	

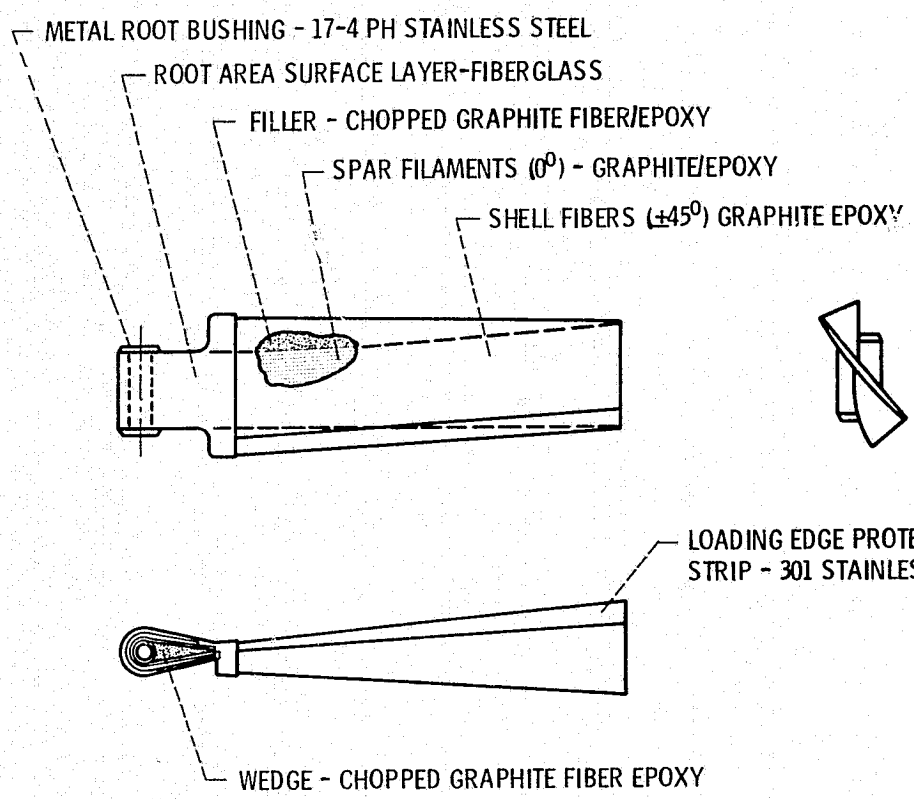

Figure 1. - Blade construction.

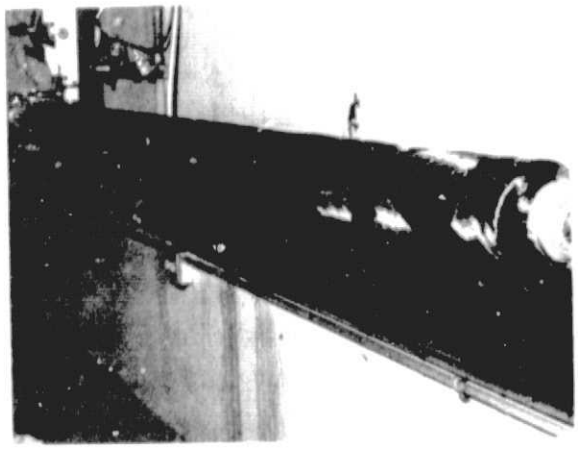

Figure 2. - Shell winding.

C-75-711

Figure 3. - Blades after curing and trimming.

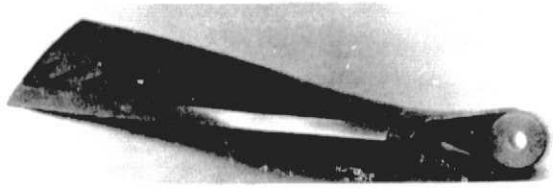

Figure 4. - Finished blade.

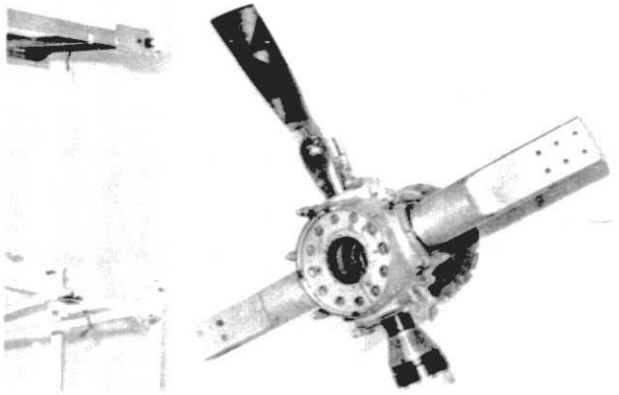

Figure 5. - Filament wound blade installed in whirl rig.

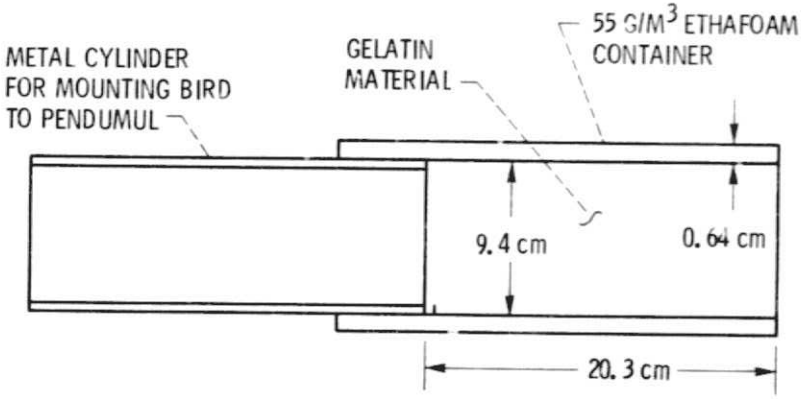

Figure 6. - Simulated bird configuration.

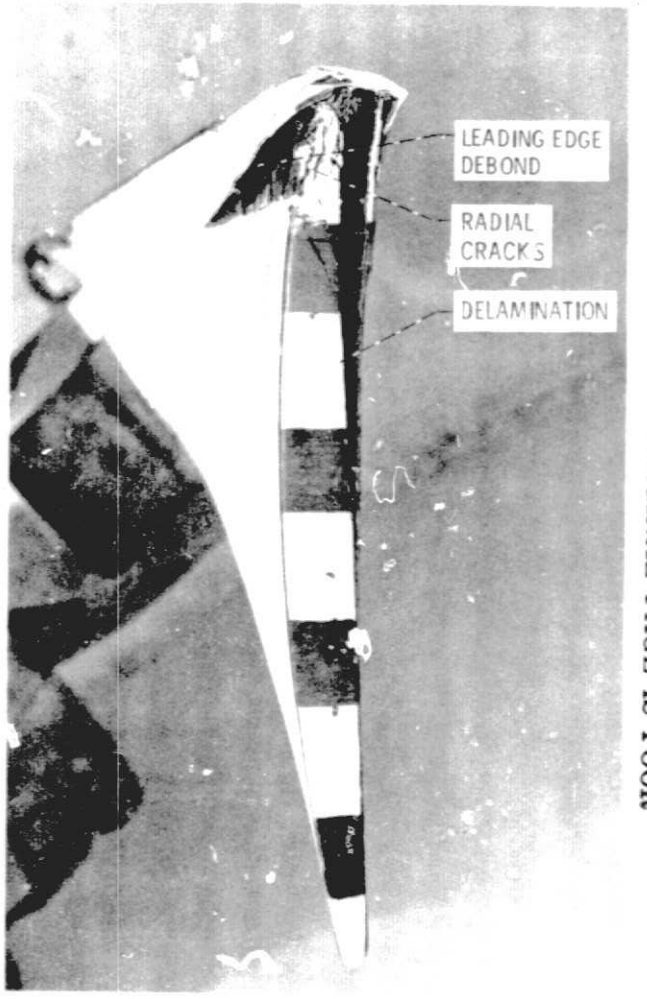

Figure 7. - Blade FS-3 after striking bird injection apparatus stand.

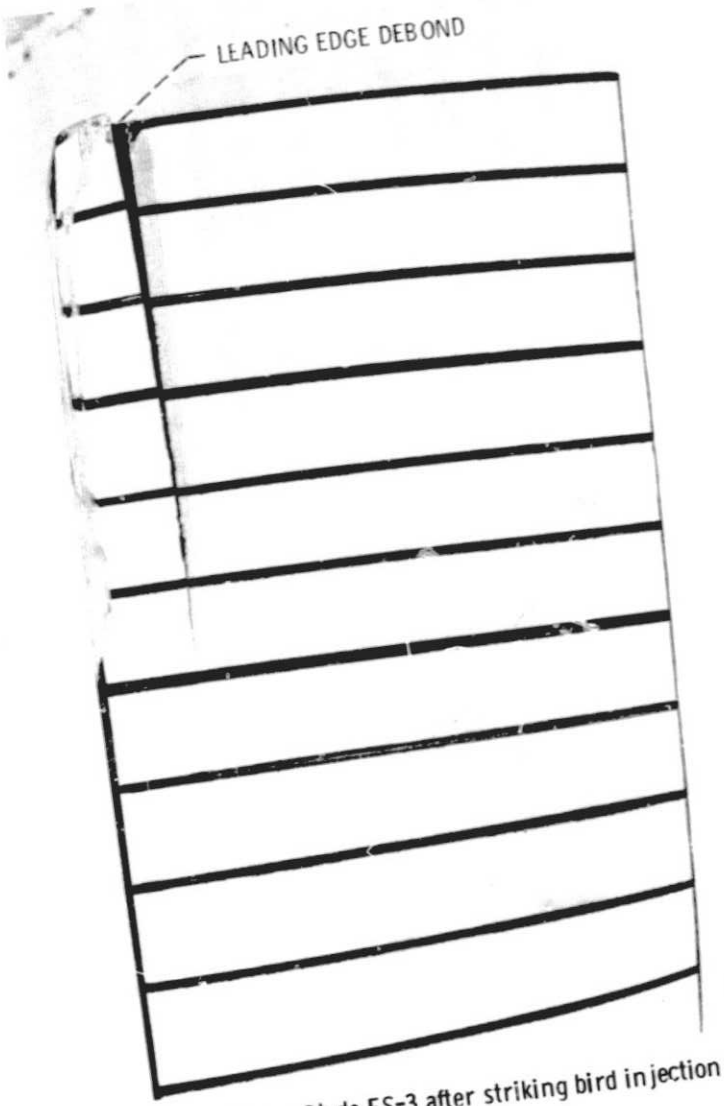

Figure 8. - Blade FS-3 after striking bird injection apparatus stand, suction side.

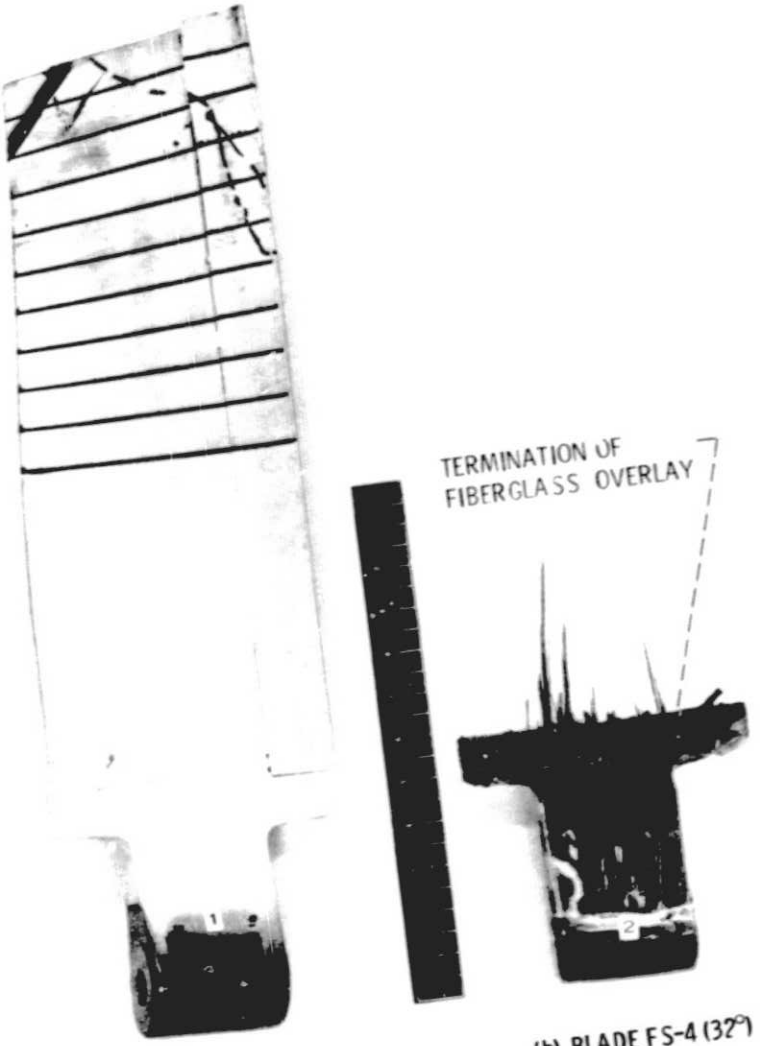

(a) BLADE FS-3 (22°)

(b) BLADE FS-4 (32°)

Figure 9. - Blade post impact condition, pressure side. Dashed line denotes boundary of initial delamination from accidental impact.

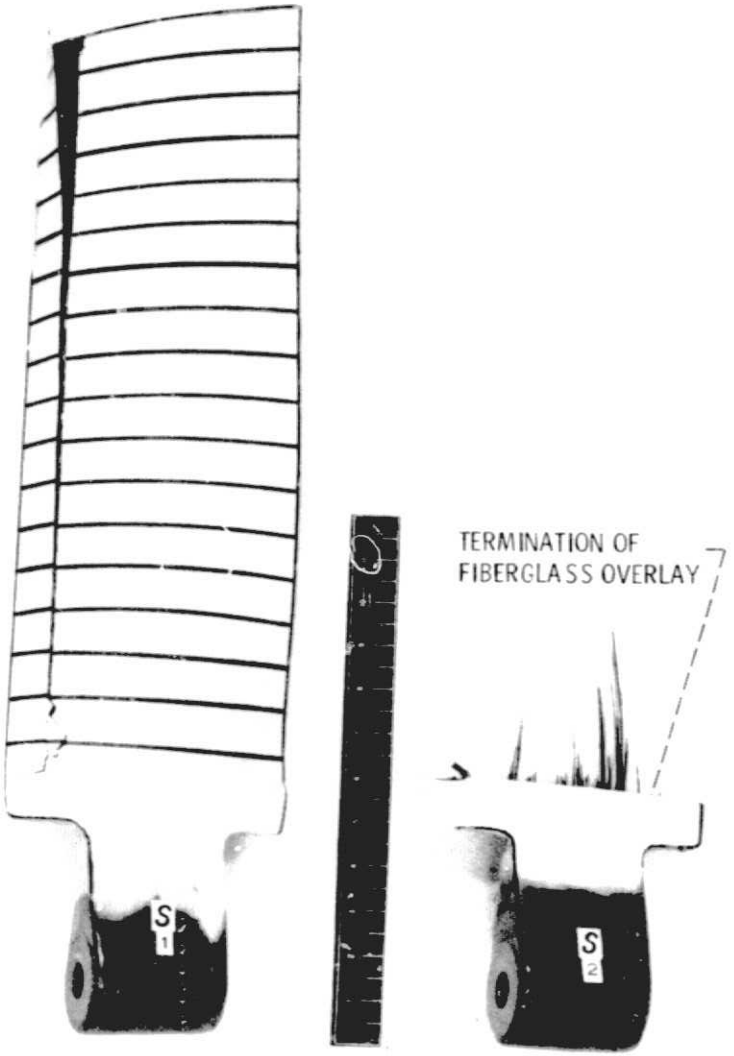

(a) BLADE FS-3 (22°) (b) BLADE FS-4 (32°)

Figure 10. - Blade post impact condition, suction side.

Figure 11. - Blade FS-3 tip post impact condition, 22° incidence angle.

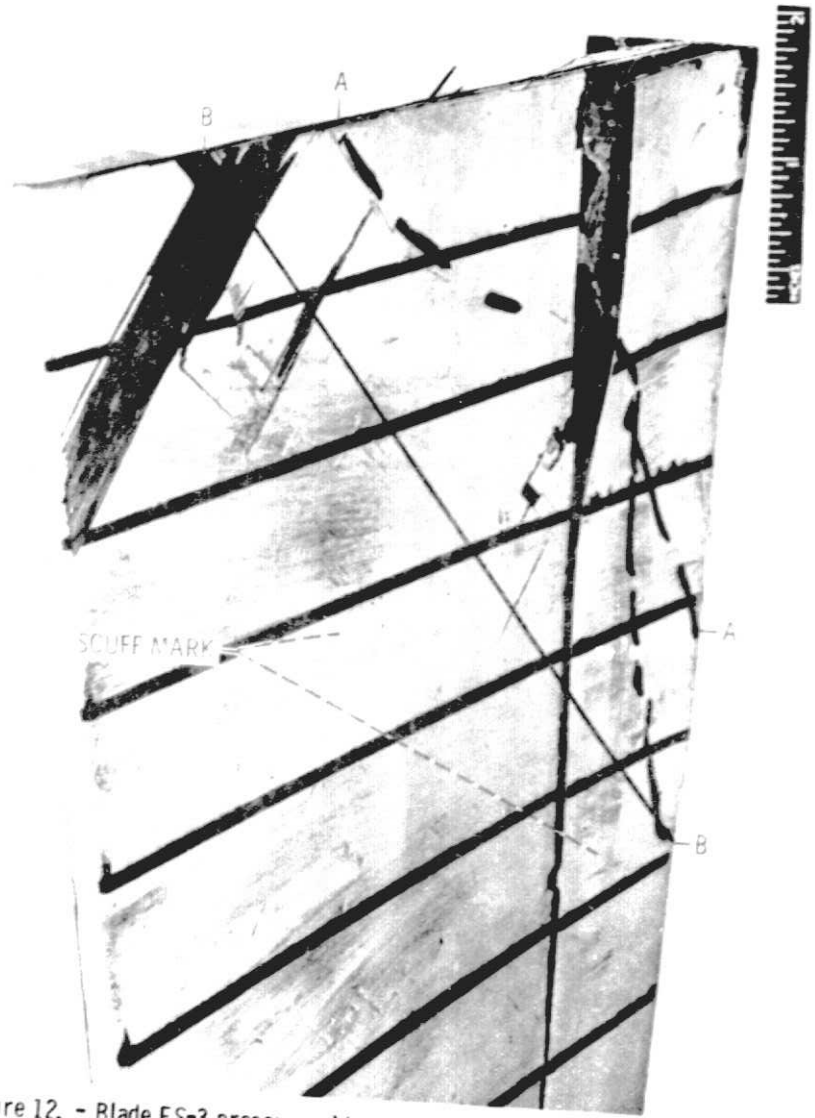

Figure 12. - Blade FS-3 pressure side post impact condition, 22° incidence angle. Line A-A is extent of delamination after accidental impact. Line B-B is extent of delamination after impact with bird.

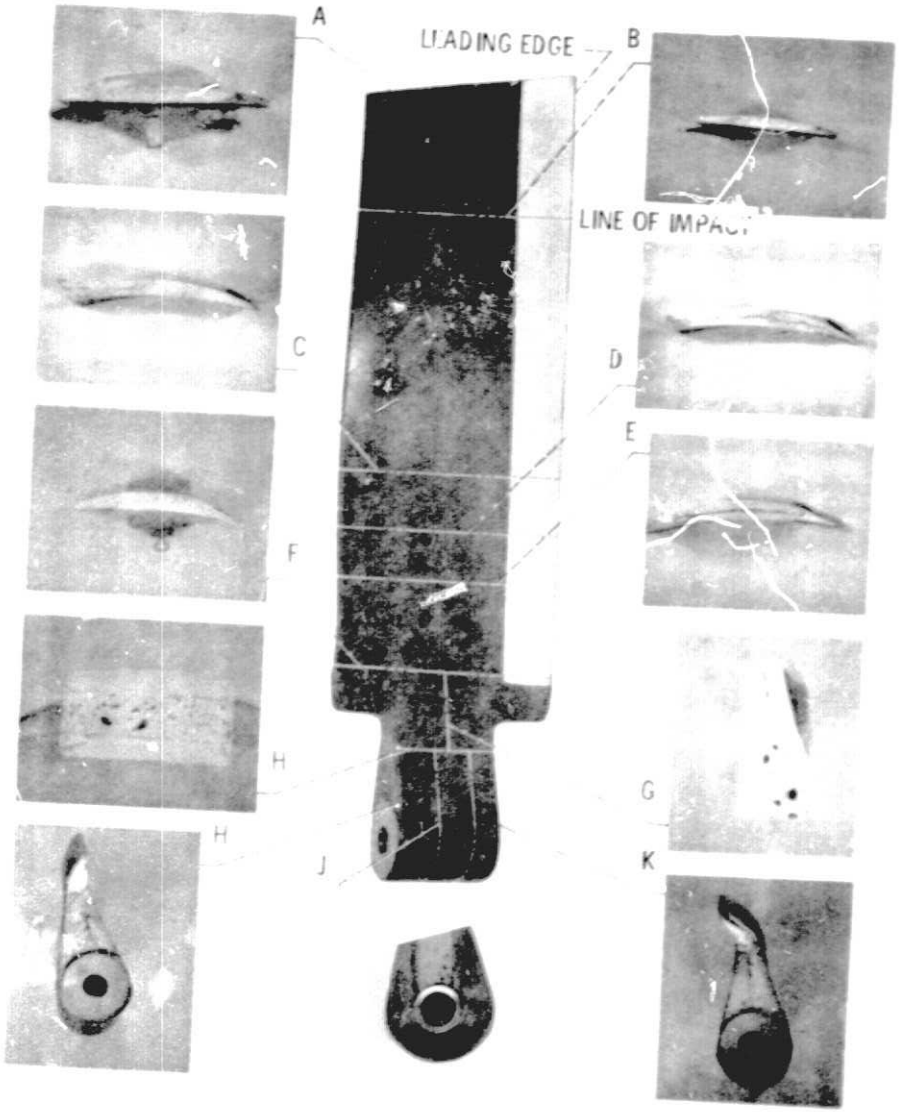

Figure 13. - Sections of Blade FS-3 after 22° impact.

Figure 14. - Pressure side of root section of blade FS-4 32° incidence angle.

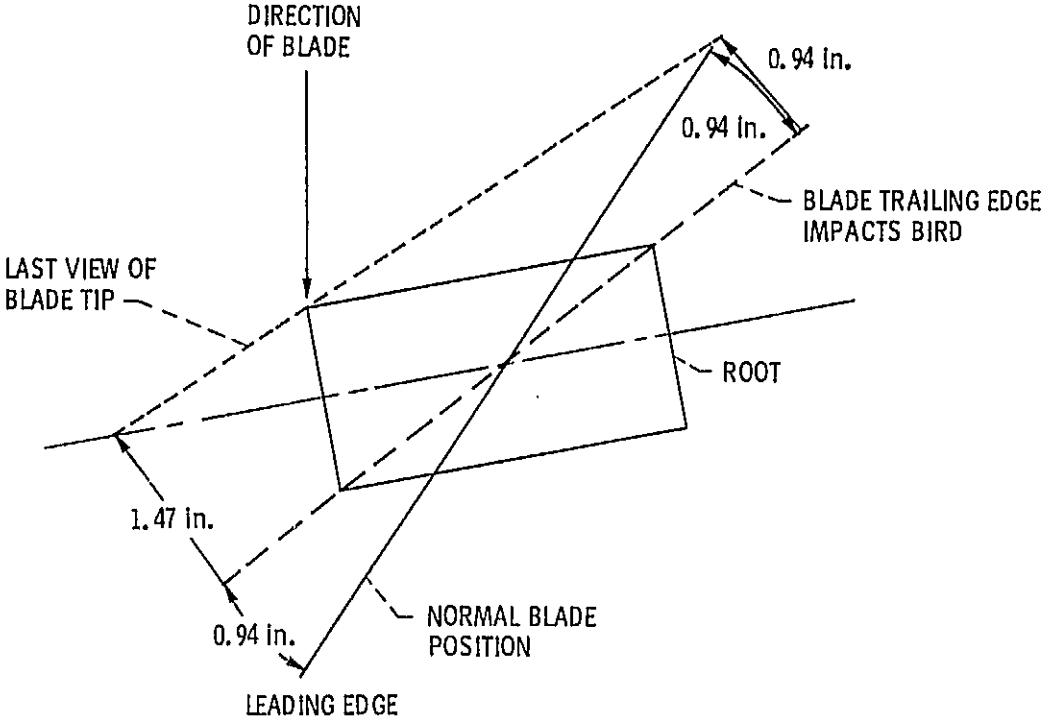

Figure 15. - Reaction of blade tip of FS-4 with simulated bird at 32^{0}.